Modeling, Identification, Estimation and Adaptation for the Control of Power Generating Kites

Roy S. Smith

Automatic Control Laboratory
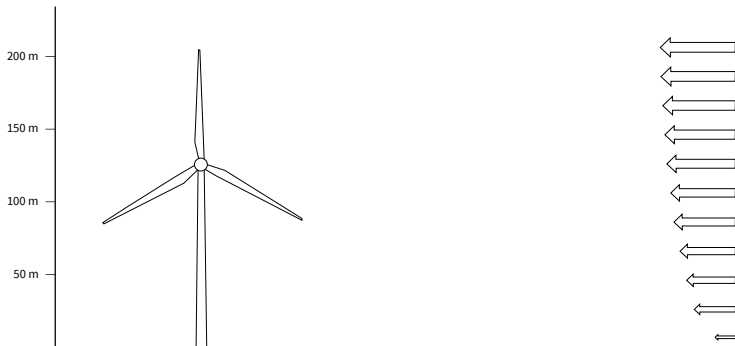ETH Zürich
rsmith@control.ee.ethz.ch

11th July 2018

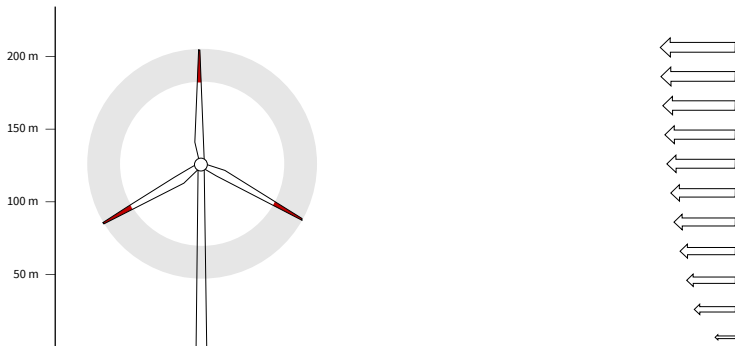18th IFAC Symposium on System Identification
Stockholm, Sweden

Motivation

▶ Winds are stronger and more consistent wind at higher altitudes;

Motivation

- Winds are stronger and more consistent wind at higher altitudes;
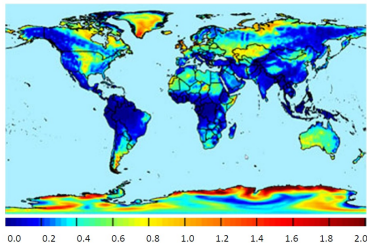- Most of the power is generated by a small part of the turbine;
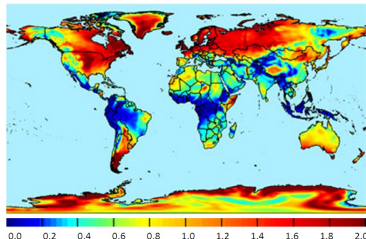
Airborne Wind Energy

Motivation

▶ Winds are stronger and more consistent wind at higher altitudes;

▶ Most of the power is generated by a small part of the turbine;

▶ Replace the effective part of the blade by a kite.

Airborne Wind Energy
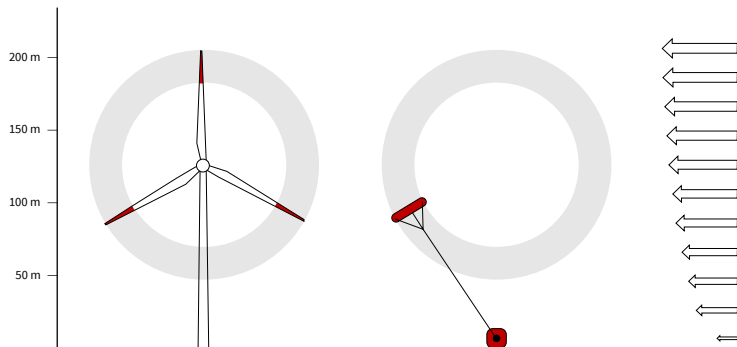
Utilization benefits

Wind power density (kW/m^2)
at 120 m. altitude.

Wind power density (kW/m^2)
at 600 m. altitude.

▶ The wind power scales with the cube of the wind velocity.

Basic concept

E 80 – 018

100 29

# Crosswind Kite Power

Miles L. Loyd*

Lawrence Livermore National Laboratory, Livermore, Calif.

This paper describes a concept for large-scale wind power production by means of aerodynamically efficient kites. Based on aircraft construction, these kites fly transverse to the wind at high speed. The lift produced at this speed is sufficient to both support the kite and generate power. The equations of motion are developed, and examples are presented. One version, based on the C-5A aircraft, results in 6.7 MW produced by a 10-m/s wind. Extrapolation to newer technology, which is more comparable to modern wind turbines, indicates the production of 45 MW from a single machine. The detailed calculations are validated by comparison of their results with simple analytical models. The methodology used here lays the foundation for the systematic study of power-producing kites.

Airborne wind energy

An abbreviated history

1980 M. Loyd, "Crosswind kite power," *J. Energy*.

2001 M. Diehl, *Real Time Optimization for Large Scale Nonlinear Processes*.

2001 W. Ockels, "Laddermill, a novel concept to exploit the energy in the airspace," *Aircraft Design*.

2005 B. Lansdorp, & W. Ockels, "Design of a 100 MW laddermill for wind energy generation from 5 km altitude," *Recovery Recycling and Reintegration*.

2006 B. Houska & M. Diehl, "Optimal control of towing kites," *CDC*.

2007 M. Canale, L. Fagiano, & M. Milanese, "Power kites for wind energy generation," *CSM*.

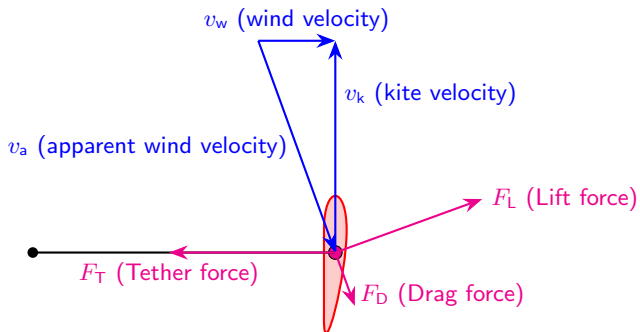2009 L. Fagiano, *Control of tethered airfoils for high-altitude wind energy generation*.

2010 · · ·

Basic aerodynamics

Lift and drag force equilibrium
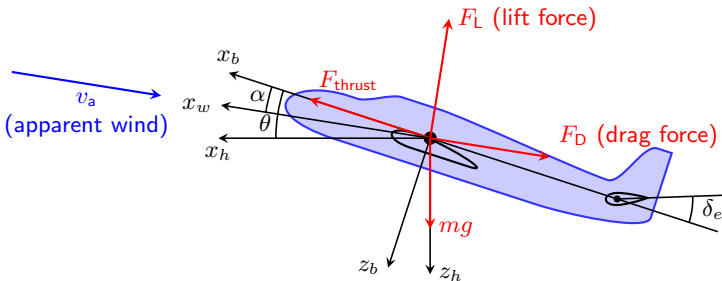
Force balance: $F_{\text{thrust}} + F_{\text{L}} + F_{\text{D}} + mg = 0$

$$\|F_{\text{L}}\| = \frac{\rho \|v_{\text{a}}\|^2}{2} C_{\text{L}} S \quad \text{and} \quad \|F_{\text{D}}\| = \frac{\rho \|v_{\text{a}}\|^2}{2} C_{\text{D}} S.$$
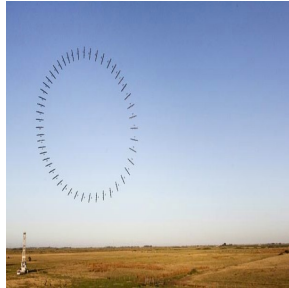
Cross-wind flight

On-board generation

Turbines/generators mounted on a rigid wing

Makani

Makani

Generation concept

- ▶ The kite is flown in a tethered cross-wind pattern.
- ▶ This kite speed is 5 to 10 times the wind speed.
- ▶ On-board propellor-driven generators are driven by the higher velocity apparent wind.

Ground-based generation

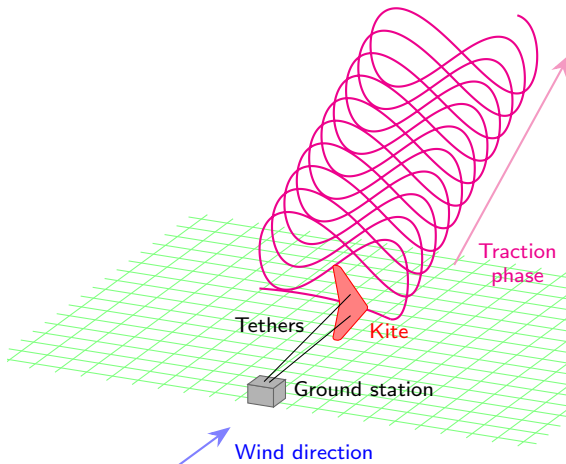## Two-phase operation

Fagiano, 2009

C. Houle, FHNW

TwingTec

Generation concept

- Kite speeds in cross-wind flight are 5 to 10 times the wind speed.
- The tethers are wound on a winch connected to a motor/generator system.
- Two phase flight is required:
  - Traction generates power;
  - Retraction consumes power.
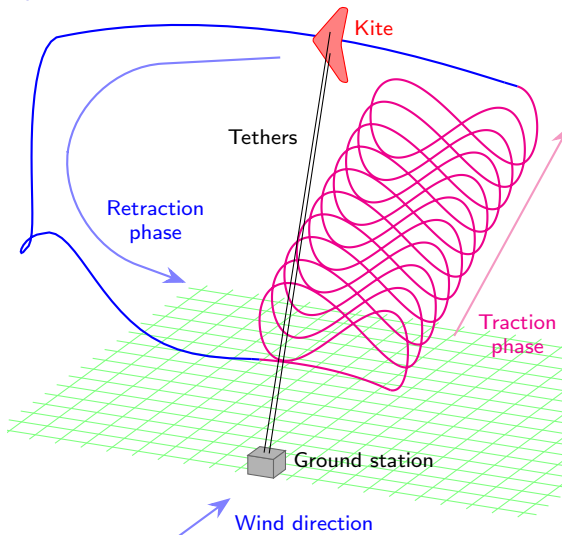
Two-phase operation

Two-phase operation

Kite

Tethers

Retraction phase

Traction phase

Ground station

Wind direction

Ground-based control and generation

Ground-based control and generation

▶ Connection to the kite via tethers.

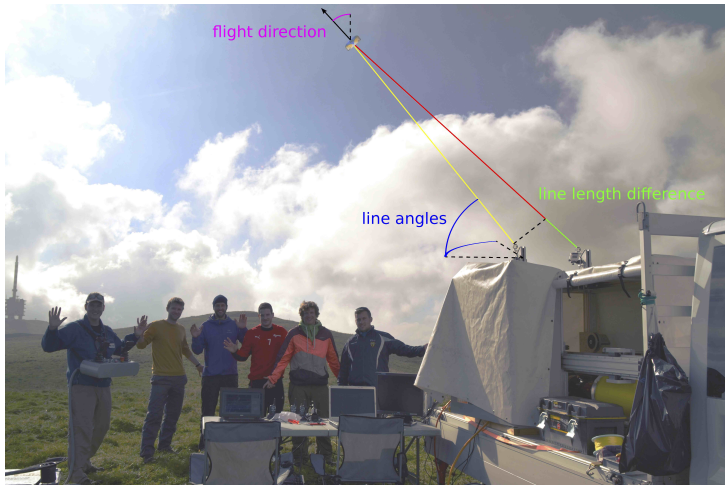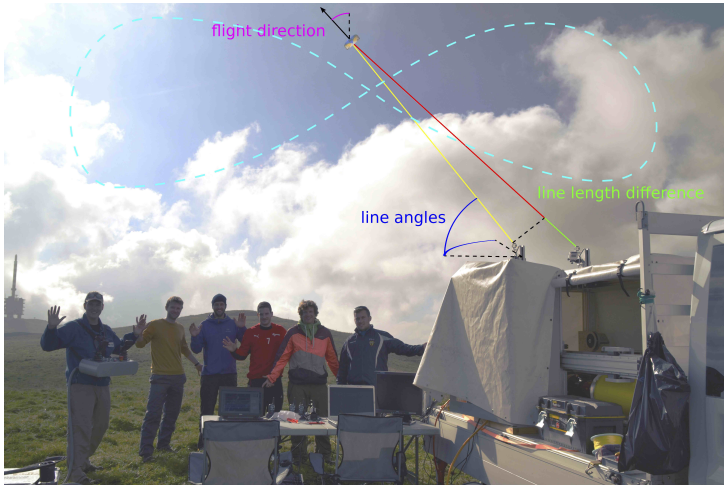# Ground-based control and generation

line length difference

- ▶ Connection to the kite via tethers.
- ▶ Actuation and sensing on the ground.

Ground-based control and generation

- Connection to the kite via tethers.
- Actuation and sensing on the ground.

- Connection to the kite via tethers.
- Actuation and sensing on the ground.
- Control of flight direction to follow a figure-of-eight path.

Ground-based control and generation

- Connection to the kite via tethers.
- Actuation and sensing on the ground.
- Control of flight direction to follow a figure-of-eight path.

Ground-based generation: pumping cycles

Configuration options

Power generation

	On-board generation	Ground-based generation
Wing:	rigid	rigid or soft
Flight path:	simple	pumping cycle
Lifting actuation:	turbines can actuate	requires additional actuators
Mass:	heavy	light weight
Crashes:	very expensive	depends on the wing structure

Wing structure

|	Rigid wings	Soft wings
Actuation:	on-board	ground-based
Sensing:	reasonably good	limited
Control performance:	high	constrained
Aerodynamics:	well modeled	highly variable
Efficiency	high	moderate
Crashes:	moderately expensive	no big deal

Focus of today's talk

1. Ground-based generation
   - Traction/retraction trajectories
   - Focus on traction phase

2. Soft kites
   - Actuation via tethers controlled from the ground.
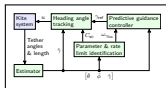   - Uncertain aerodynamics
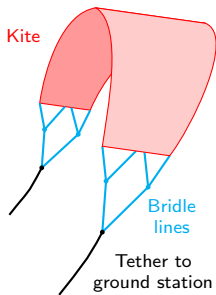
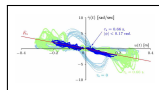

Kite

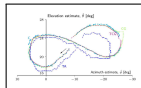Bridle lines

Tether to ground station

Modeling

Control architecture

Parameter estimation

State estimation

Control experiments

Modeling

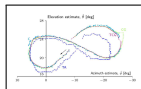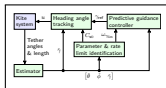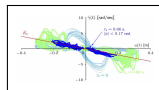Control architecture

Parameter estimation

State estimation

Control experiments

Coordinates
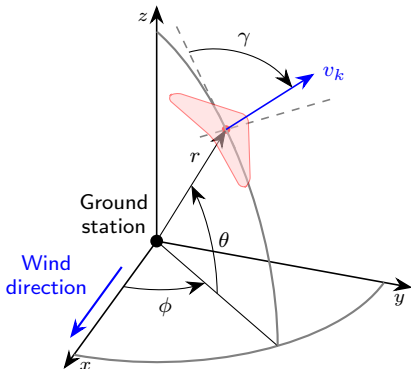
The wind direction defines the x-axis.

ϕ	Azimuth angle
θ	Elevation angle
γ	flight path heading angle
v_k	kite velocity
r	tether length

Simplifying assumption

1. Slow reel-out ($\dot{r}(t) \ll v_\mathsf{k}$).

Kinematic model

$$\dot{\theta} = \frac{v_{\mathsf{k}}}{r} \cos \gamma, \quad \text{and} \quad \dot{\phi} = \frac{v_{\mathsf{k}}}{r \cos \theta} \sin \gamma \qquad (\text{assumes } \dot{r} = 0)$$

Flight path angle

$$\gamma = \arctan \left(\frac{\cos(\theta) \, \dot{\phi}}{\dot{\theta}} \right)$$

Actuation model

The actuation model is motivated by the data.

$$\dot{\gamma} = K_{\mathsf{s}} \, u(t - \tau_{\mathsf{s}}) \qquad (u \text{ is the tether length difference}).$$

Actuation model from: Erhard & Strauch, *TCST*, 2013

Basic aerodynamics

Simplifying assumptions

1. Slow reel-out ($\dot{r}(t) \ll v_k$).
2. Low kite mass (force equilibrium).
3. Neglect tether mass, drag and dynamics.

Apparent wind

$$v_a = v_w - v_k,$$

Determines the aerodynamic forces:

$$\|F_L\| = \frac{\rho\|v_a\|^2}{2}C_L S$$

$$\|F_D\| = \frac{\rho\|v_a\|^2}{2}C_D S$$

Basic aerodynamics
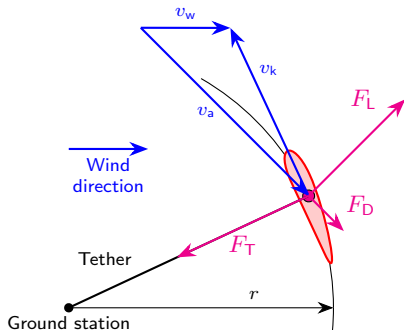
Kite speed

Starting from apparent wind:

$$\|v_{a_{\text{tangential}}}\| \;=\; \|v_\text{w}\|\frac{C_\text{L}}{C_\text{D}}\cos\theta\,\cos\phi.$$

For efficient (high C_L/C_D) kites:

$$\|v_\text{k}\| \;\approx\; \|v_\text{w}\|\frac{C_\text{L}}{C_\text{D}}\cos\theta\,\cos\phi.$$

More and better models: Schmehl, R., Noom, M., and van der Vlugt, R., Springer, 2013.

Modeling: aerodynamics

Approximate model

$$\dot{\theta} = \frac{v_{\mathsf{k}}}{r} \cos \gamma$$

$$\dot{\phi} = \frac{v_{\mathsf{k}}}{r \cos \theta} \sin \gamma$$

$$\dot{\gamma} = K_{\mathsf{s}} \, u(t - \tau_{\mathsf{s}})$$

$$\|v_{\mathsf{k}}\| \approx \|v_{\mathsf{w}}\| \frac{C_{\mathsf{L}}}{C_{\mathsf{D}}} \cos \theta \, \cos \phi.$$

Sources of uncertainty

► For soft kites C_{L} and C_{D} are uncertain and variable (particularly when turning).

► v_{w} is not accurately known as a function of altitude.

► v_{w} can vary quickly and significantly in magnitude and direction.

► K_{s} varies (particularly with v_{k}) due to tether dynamics.

► τ_{s} varies (particularly with r and F_{T}) due to tether dynamics.

An outline
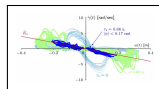
Modeling
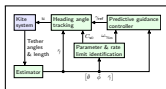
Control architecture
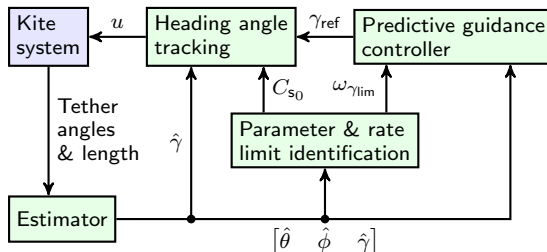

Parameter estimation

State estimation
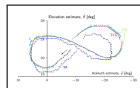
Control experiments

Cascade control structure

Guidance:	Heading angle trajectory generation	
	Traction phase power extraction	
Tracking:	Track heading angle, γ_{ref}	
	Compensate for gain and delay variation	
Identification:	Estimate gain, K_{s}, and delay, τ_{s}, for each figure-of-eight cycle.	

Cascaded structures are also in: Erhard & Strauch, *TCST*, 2013; Jehle & Schmehl, *JGCD*, 2014; Fagiano, Zgraggen, Morari & Khammash, *TCST*, 2014
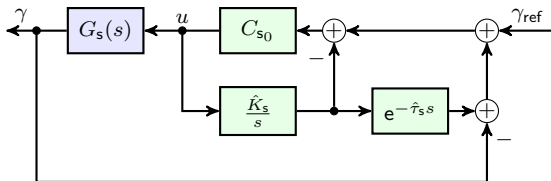
Delayed plant model

$$\gamma = G_{\mathsf{s}}(s)u = \frac{K_{\mathsf{s}}}{s}\mathsf{e}^{-\tau_{\mathsf{s}}s}u.$$

▶ The steering delay, τ_{s}, ranges between 0.5 and 2 seconds.

Smith predictor configuration

Smith predictor configuration

Design an ideal loopshape:

$$\frac{C_{s_0} K_s}{s} e^{-\tau_s s} \qquad (C_{s_0} \text{ constant})$$

Smith predictor controller uses estimates of K_s and τ_s:

$$C_s(s) = \frac{C_{s_0}}{1 + \frac{C_{s_0} \hat{K}_s}{s}(1 - e^{-\hat{\tau}_s s})}$$

Inner loop control: Heading angle tracking

Robustness requirements

Uncertain steering gain, $K_{\sf s}$, and steering delay, $\tau_{\sf s}$:

$$\hat{K}_{\sf s} - \delta_{K_{\sf s}} < K_{\sf s} < \hat{K}_{\sf s} + \delta_{K_{\sf s}} \qquad\qquad \hat{\tau}_{\sf s} - \delta_{\tau_{\sf s}} < \tau_{\sf s} < \hat{\tau}_{\sf s} + \delta_{\tau_{\sf s}}$$

Robust stability of the Smith predictor is "guaranteed" for:

$$C_{\sf s_0} < \frac{\pi}{2\hat{K}_{\sf s}\delta_{\tau_{\sf s}}\sqrt{\left(1 + \frac{\delta_{K_{\sf s}}}{\hat{K}_{\sf s}}\right)^2 + 1}},$$

Bandwidth limits

Guidance limitation,

$$|\dot{\gamma}_{\sf ref}| < \omega_{\gamma_{\sf lim}}, \qquad \text{(depends on } C_{\sf s_0}, \hat{K}_{\sf s}, \text{ and } \hat{\tau}_{\sf s})$$

imposed by the predictive guidance algorithm.

See: Wood, Hesse, Zgraggen, & Smith, *CDC*, 2015.

Model predictive control: generating γ_{ref}

- ▶ Generate (v_{w}, r) parameterized family of trajectories.

- ▶ Relatively standard (quadratic) MPC for state-deviation

  - Soft constraints on the position errors.
  - Include $\omega_{\gamma_{\text{lim}}}$ bandwidth constraint.
  - Account for τ_{s} delay: predict using past inputs.
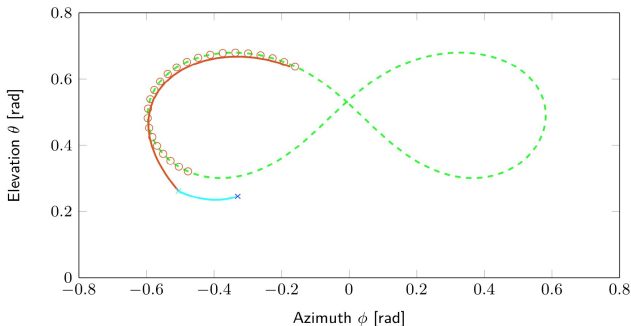
Offline trajectory generation

$$
\begin{aligned}
\operatorname*{maximize}_{x(\cdot),u(\cdot),x_0,T_{\mathsf{p}}} \quad & \frac{1}{T_{\mathsf{p}}} \int_0^{T_{\mathsf{p}}} F(x(t),u(t))dt \\
\text{subject to:} \quad & \dot{x} = f(x(t),u(t)) && \text{(dynamics)} \\
\forall t \in [0,T_{\mathsf{p}}] \quad & \underline{c} \le x(t) \le \overline{c} && \text{(altitude limits)} \\
& \underline{b} \le u(t) \le \overline{b} && \text{(actuation limits)} \\
& x(0) = x(T_{\mathsf{p}}) = x_0 && \text{(periodicity)}
\end{aligned}
$$

Objective function

Approximation of the tether force, F_{T}:

$$
F(x,u) = \frac{\rho S C_{\mathsf{D}}}{2} \left(1 + \left(\frac{C_{\mathsf{L}}}{C_{\mathsf{D}}} - \beta u^2 \right)^2 \right)^{3/2} (\cos\theta \, \cos\phi \, v_{\mathsf{w}})^2
$$

An outline

Modeling
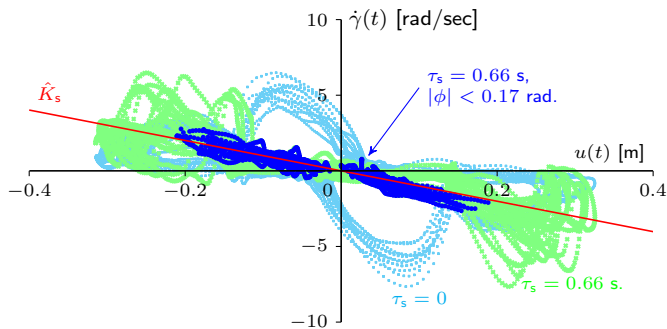

Control architecture

Parameter estimation
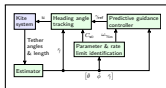
State estimation
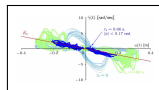
Control experiments
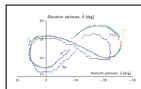
Parameter estimation

Steering gain parameter estimation

Actuation model: $\dot{\gamma} = K_{\mathsf{s}}\, u(t - \tau_{\mathsf{s}})$

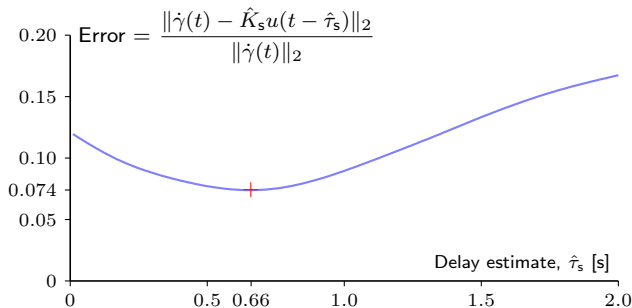An estimate of $\dot{\gamma}$ comes from an Inertia Measurement Unit (IMU) on the kite.

Steering delay parameter estimation

Actuation model: $\qquad \dot{\gamma} = K_{\mathsf{s}}\, u(t - \tau_{\mathsf{s}})$

Best gain fit, $\hat{K}_{\mathsf{s}}$, as a function of the estimated delay, $\hat{\tau}_{\mathsf{s}}$.
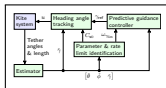
An outline

Modeling
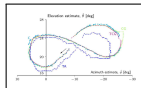
Control architecture

Parameter estimation

State estimation
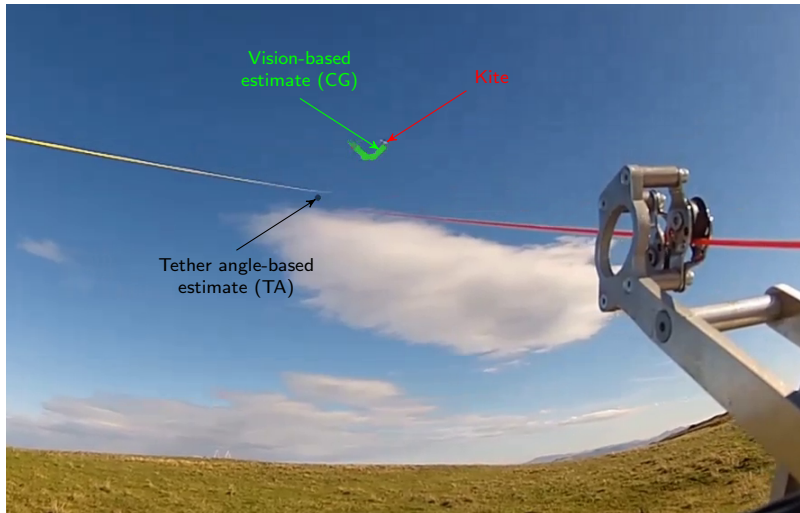

Control experiments

Challenges

Sensing options

Tether angle sensing. Encoders mounted on the tether feed-out arms.

Inertial measurement unit (IMU). Mounted on the kite.
(3-axis accelerometer, 3-axis gyroscope).

Vision sensing. Video camera on the tether feed-out arms.
(1280×960 pixels, 48 frames/second).

Radio localisation. Ultra-wide band time-of-flight radio sensors on the kite.
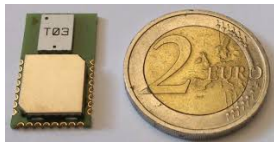
Range: 290 m.
Accuracy: 0.1 m
Update rate: 50 Hz.

GPS position measurements are not feasible.

Estimator/sensor configurations

Name	Process model	Sensing
TA	Unicycle	tether angles/gyro
CG	Unicycle	camera/gyro
TCG	Dual unicycle	tethers/camera/gyro

Estimator model assumptions: unicycle

1. The tethers are rigid (and have no mass or drag).
2. The camera gives direct (undelayed) measurements of θ and ϕ.
3. The gyroscope rate measurements of θ and ϕ contain noise and drift which is included in the estimated variables.

Dual-unicycle model

Create a second unicycle model,

$$\dot{\theta}^* \;=\; \frac{v_{\mathsf{k}}^*}{r}\cos\gamma^* \qquad \text{and} \qquad \dot{\phi}^* \;=\; \frac{v_{\mathsf{k}}^*}{r\,\cos\theta^*}\sin\gamma^*,$$

The (θ^*,ϕ^*) model is coupled to the (θ,ϕ,γ) kite model via,

$$v_{\mathsf{k}}^* \;=\; v_{\mathsf{k}} - v_{\mathsf{offset}} \qquad \text{and} \qquad \gamma^* \;=\; \lambda\gamma(t - t_{\mathsf{offset}}) \qquad (\text{with } \lambda \approx 1).$$

The parameters v_{offset} and t_{offset} can be estimated offline from prior data.

Estimator model assumptions: dual unicycle

1. The tethers are rigid (and have no mass or drag) and give direct (undelayed) measurements of θ^* and ϕ^*.

2. The camera gives direct (undelayed) measurements of θ and ϕ.

3. The gyroscope rate measurements of θ and ϕ contain noise and drift which is included in the estimated variables.

Post-analysis of video flight data

Estimation

Estimator comparison: $\hat\theta$, $\hat\phi$
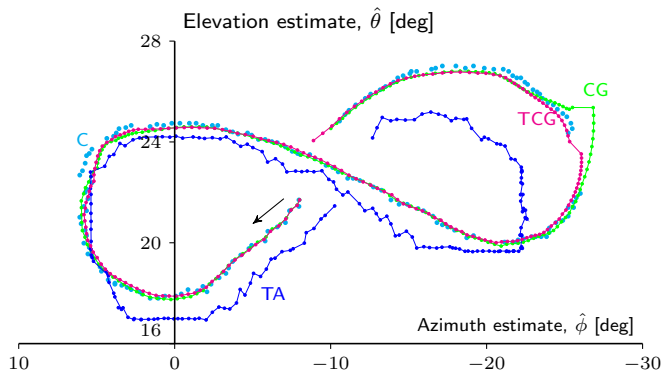
TA estimates

CG estimates

Camera measurements

TGC estimates

Estimation

Estimator comparison: $\hat{\gamma}$

Heading angle estimate, $\hat{\gamma}$ [deg]

TA estimates   CG estimates   TGC estimates
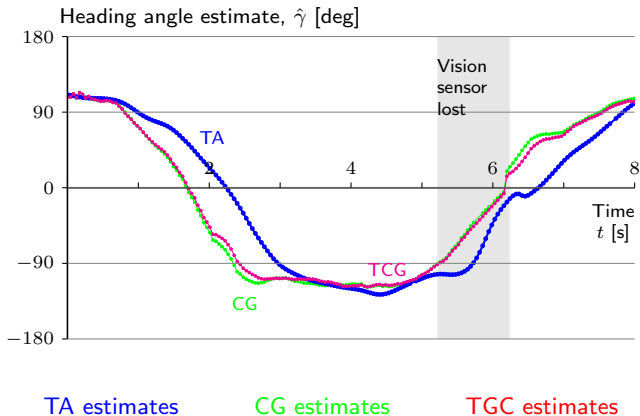
Estimator comparison: using post analysis on video flight data

| Name	Process model	Sensing	$\hat{\gamma}$ error [deg.]	$(\hat{\theta}, \hat{\phi})$ error [deg.]
TA	Unicycle	tether angles/gyro	21	4.1
CG	Unicycle	camera/gyro	11	0.7
TCG	Dual unicycle	tethers/camera/gyro	9.7	0.7

▶ The camera gives a very large improvement in position accuracy.

▶ For heading angle the camera reduces the error by half (w.r.t. TA)

▶ The combination of tether angles and camera provides some additional heading angle estimation improvement.
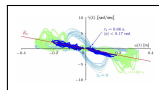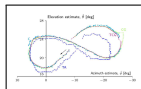
An outline

Modeling

Control architecture
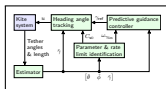
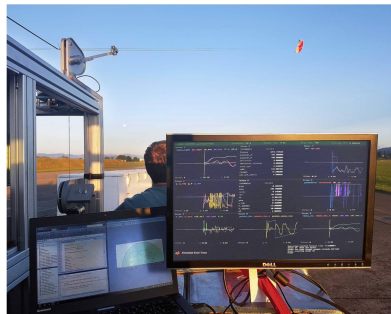Parameter estimation

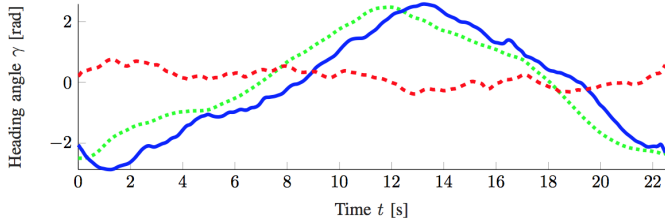State estimation

Control experiments

Tow testing

- ▶ 5 m^2 kite.
- ▶ Sampling time: 10 milliseconds.
- ▶ MPC prediction horizon: 30 steps (0.3 seconds).
- ▶ Figure-of-eight cycle period: approx. 20 seconds.

Path tracking performance: γ

Inner loop (heading angle) tracking control

Reference: γ_{ref} Tracking: γ path

Tracking error, $\gamma - \gamma_{\text{ref}}(t - \tau_{\text{s}})$

► The γ_{ref} tracking controller (Smith predictor) tracks the delayed reference.

Path tracking performance: (θ, ϕ)

Model predictive controller for guidance

Single cycle example:
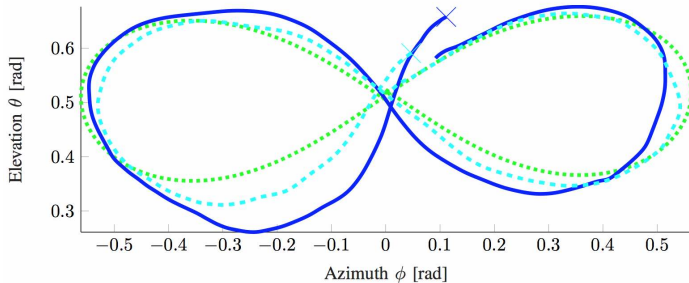
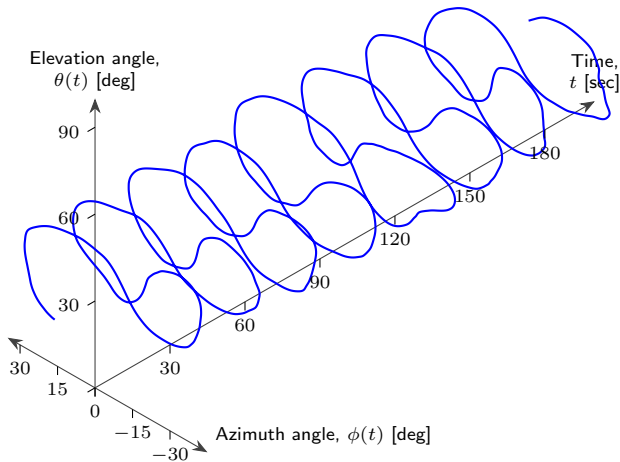Reference path   Tracking (with non-predictive guidance)

                            Tracking (with predictive guidance)

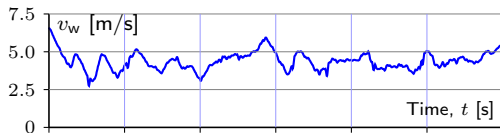Adaptive Smith-predictor/Model predictive control cascade
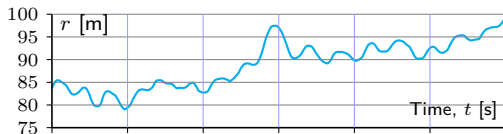
Figures-of-eight

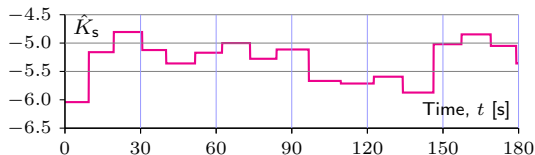# Experimental adaptive control

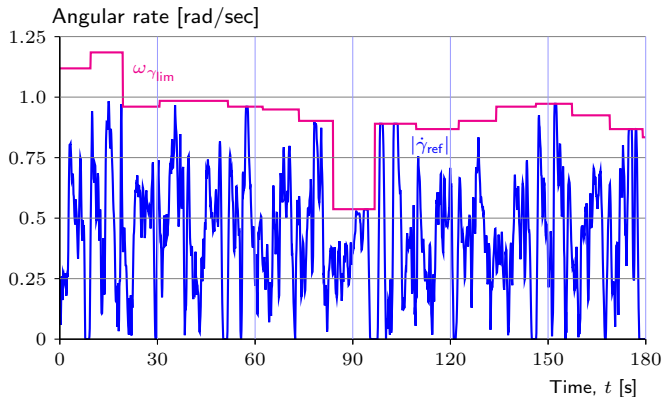Wind speed measurement

Tether length measurement

Steering delay estimate

Steering gain estimate

Experimental adaptive control
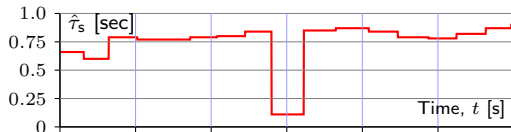
Adaptive bandwidth limitation

- The MPC guidance controller respects the bandwidth limitation.
- The actual turn rate comes close to the bound.

Discussion

White box identification problem

- ▶ How detailed should the model be?

    - What is needed for the control task?

    - What behaviours/dynamics are reliably reproduced by the model?

    - Finding the tradeoff between model complexity, model reliability, robustness, control performance.

- ▶ Identifying the parameters:

    - Which should be identified offline by experiment?
      $(C_D, C_L, \beta, t_{offset}, v_{offset})$

    - Which should be estimated online and used for adaptation?
      (K_s, τ_s).

Really hard problems for kite control

- ▶ Reliable take off and landing.

- ▶ Robustness to a wide range of conditions.

- ▶ Long term autonomy.

The future?

Almost commercial technologies

Makani, US
600 kW

TwingTec, Switzerland
50 kW

Skysails, Germany
160 m^2 kite

Ampyx, Netherlands

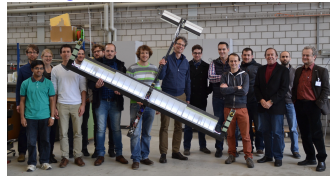

KiteGen, Italy

EnerKite, Germany

Acknowledgments

ETH, Automatic Control Lab

Eva Ahbe, RS, Tony Wood, Henrik Hesse,
Lorenzo Fagiano, Max Polzin,
Aldo Zgraggen, Manfred Morari.

TwingTec collaboration

Rolf Lucksinger, Corey Houle
Colin Jones (EPFL)

AWESCO Project

Roland Schmehl (TU Delft) *et al.*

Thanks for your attention.

References

▶ T.A. Wood, H. Hesse, A.U. Zgraggen, & R.S. Smith, "Model-based identification and control of the velocity vector orientation for autonomous kites," *Proc. ACC,* 2377–2382, 2015.

▶ A. Millane, H. Hesse, T.A. Wood, & R.S. Smith, "Range-inertial estimation for airborne wind energy," *Proc. IEEE CDC,* 455–460, 2015.

▶ T.A. Wood, H. Hesse, A.U. Zgraggen, & R.S. Smith, "Model-based flight path planning and tracking for tethered wings," *Proc. IEEE CDC,* 6712–6717, 2015.

▶ T.A. Wood, E. Ahbe, H. Hesse, & R.S. Smith, "Predictive guidance control for autonomous kites with input delay," *Proc. IFAC WC,* 13276–13281, 2017.

▶ M. Polzin, T.A. Wood, H. Hesse, & R.S. Smith, "State estimation for kite power systems with delayed sensor measurements," *Proc. IFAC WC,* 11959–11964, 2017.

▶ T.A. Wood, H. Hesse, & R.S. Smith, "Predictive control of autonomous kites in tow test experiments", *IEEE Ctrl. Syst. Letters,* **1**(1), 110–115, 2017.

▶ H. Hesse, M. Polzin, T.A. Wood, & R.S. Smith, "Visual motion tracking and sensor fusion for ground-based kite power systems", *Airborne Wind Energy*, 413–438, Springer, 2018.

▶ R. Luchsinger, D. Aregger, F. Bezard, D. Costa, C. Galliot, F. Gohl, J. Heilmann, H. Hesse, C. Houle, T.A. Wood, & R.S. Smith, "Kite power with Twings," *Airborne Wind Energy,* 603–621, Springer, 2018.

▶ E. Ahbe, T.A. Wood, & R.S. Smith, "Stability verification for periodic trajectories of autonomous kite power systems," *ECC,* 2018.